The C-terminal PDZ-ligand motif of the neuronal glycine transporter GlyT2 is required for efficient synaptic localization

Wencke Armsen, Bettina Himmel, Heinrich Betz, Volker Eulenburg

The C-terminal PDZ-ligand motif of the neuronal glycine transporter GlyT2 is required for efficient synaptic localization

Wencke Armsen,[a,1] Bettina Himmel,[a,b] Heinrich Betz,[a,*] and Volker Eulenburg[a]

[a]Department of Neurochemistry, Max-Planck Institute for Brain Research, Deutschordenstrasse 46, 60528 Frankfurt am Main, Germany
[b]Department of Biophysical Chemistry, Max-Planck Institute of Biophysics, Max-von-Laue Str. 3, 60438 Frankfurt am Main, Germany

Introduction

Glycine is the major inhibitory neurotransmitter of interneurons in spinal cord and brain stem, where it activates strychnine-sensitive postsynaptic glycine receptors (Betz and Laube, 2006; Lynch, 2004). To allow for high-frequency synaptic transmission, glycine concentrations in the synaptic cleft have to be tightly regulated. This is accomplished by two high-affinity glycine transporters (GlyTs), GlyT1 and GlyT2 (Liu et al., 1992; Lopez-Corcuera et al., 1991; Smith et al., 1992). The GlyTs belong to the *SLC6a* family of Na$^+$/Cl$^-$-dependent neurotransmitter transporters, which share a common topology with twelve transmembrane domains and intracellular N- and C-termini (Eulenburg et al., 2005; Gether et al., 2006). The transmembrane domains 3 and 4 are connected by a large extracellular loop that harbors multiple N-glycosylation sites (Martinez-

* Corresponding author. Fax: +49 69 96769441.
E-mail address: neurochemie@mpih-frankfurt.mpg.de (H. Betz).
[1] Current address: Department of Neurology, Children's Hospital Boston, Harvard Medical School, 300, Longwood Avenue, Boston, MA 02115, USA.

Maza et al., 2001). Although GlyT1 and GlyT2 share overlapping expression domains in caudal regions of the CNS, they differ in their cellular distributions. GlyT1 is a predominantly glial transporter mainly expressed by astrocytes (Adams et al., 1995; Zafra et al., 1995a,b). In addition, it has been found in glycinergic amacrine cells of the retina (Pow and Hendrickson, 1999) and, more recently, in a subset of hippocampal neurons (Cubelos et al., 2005a). In contrast, GlyT2 is concentrated at glycinergic nerve terminals in close proximity to the presynaptic release sites (Mahendrasingam et al., 2003; Zafra et al., 1995a) and constitutes the only specific marker protein of glycinergic interneurons known presently (Poyatos et al., 1997).

The importance of GlyTs for inhibitory neurotransmission has been proven by the generation of GlyT-deficient mice (Gomeza et al., 2003a,b). Their analysis disclosed that GlyT1 and GlyT2 have vital but complementary functions in the nervous system of young postnatal mice. GlyT1 is essential for the removal of glycine from the synaptic cleft and hence important for terminating glycinergic neurotransmission, whereas GlyT2 is required for the reuptake of glycine into the presynaptic terminal and its subsequent loading into synaptic vesicles by the vesicular inhibitory amino acid transporter (VIAAT). In addition to its function at inhibitory synapses, GlyT1 has been shown to be involved in the regulation of extracellular glycine concentrations at NMDA receptor containing excitatory synapses (Gabernet et al., 2005; Tsai et al., 2004; Yee et al., 2006).

Although the transport activities of both GlyTs are thought to be tightly controlled, GlyT2 appears to be subject to particular regulatory mechanisms (Eulenburg et al., 2005). Different lines of evidence indicate that the surface availability of GlyT2 determines neuronal glycine uptake activity. In synaptosomal preparations, only about 5–10% of the total GlyT2 protein are present in the plasma membrane, whereas its major fraction is localized intracellularly, most likely in vesicles (Geerlings et al., 2002). One protein involved in the regulation of GlyT2 plasma membrane insertion is syntaxin 1A, which has been found to indirectly interact with the N-terminal domain of GlyT2 (Geerlings et al., 2000). In transfected cells, coexpression of GlyT2 with syntaxin 1A results in a down-regulation of transport activity. However, in synaptosomal preparations inactivation of syntaxin 1A reduced GlyT2-mediated substrate uptake (Lopez-Corcuera et al., 2001), suggesting that syntaxin 1A is

involved in the regulation of both incorporation into and retrieval from the plasma membrane. Phorbol ester treatment causes enhanced GlyT2 internalization, showing that protein kinase C (PKC) contributes to the regulation of GlyT2 (Gomeza et al., 1995). Although direct phosphorylation of the transporter by PKC appears to be unlikely, residues required for PKC-induced down-regulation of GlyT2 have been identified within intracellular loop 2 (Fornes et al., 2004).

The presynaptic localization of GlyT2 implies that specific targeting and anchoring proteins must exist. Consistent with this view, the putative membrane trafficking protein Ulip6, a member of the unc-33 like phosphoprotein/collapsin response mediator protein family, has been reported to interact with the long N-terminal domain of GlyT2 (Horiuchi et al., 2000, 2005). In addition, the C-terminal intracellular tails of transporters of the *SLC6a* family are thought to contain motifs that are important for the trafficking and/or activity of these membrane proteins (Farhan et al., 2004). Besides residues that have been suggested to regulate protein exit from the endoplasmic reticulum, the extreme C-terminus of GlyT2 comprises a class III PDZ (postsynaptic density 95/disc large/zona occludens 1) domain binding motif (termed PDZ-ligand motif here) to which syntenin-1, a synaptically enriched protein harboring two PDZ domains, binds (Ohno et al., 2004). In different studies, PDZ domain containing proteins have been shown to play crucial roles in the trafficking and anchoring of membrane proteins at synaptic sites (Bezprozvanny and Maximov, 2001; Kim and Sheng, 2004).

Here, we inactivated the PDZ-ligand motif of GlyT2 by either truncation or addition of an alanine at its C-terminal end. The resulting mutant transporters were indistinguishable from wild-type GlyT2 in surface expression and uptake activity but, upon expression in neuronal cells, displayed significantly reduced synaptic localization. Thus, the PDZ-ligand motif of GlyT2 is required for its efficient recruitment to or stabilization at the nerve terminal.

Results

Generation of GlyT2 expression constructs

To analyze possible functions of the GlyT2-PDZ-ligand motif, cDNAs encoding the GlyT2a and b splice variants (Ebihara et al., 2004) were amplified by PCR from mouse spinal cord and introduced into pcDNA3.1(+) for eukaryotic expression (GlyT2^{wt}). Two strategies were used to disrupt PDZ-ligand motif function, which generally requires the three C-terminal amino acids for efficient binding (Bezprozvanny and Maximov, 2001; Bjerggaard et al., 2004). First, the three C-terminal amino acids of GlyT2 known to be essential for syntenin-1 binding (Ohno et al., 2004) were deleted to generate GlyT2$^{\Delta TQC}$. Second, an alanine was added at the extreme C-terminus to result in the GlyT2^{+A} protein (Fig. 1A). Both mutations result in a complete loss of syntenin-1 binding, as shown by GST-pulldown experiments (Ohno et al., 2004; and data not shown). Additionally, we constructed N-terminal EGFP-GlyT2 fusion proteins for the wild-type transporter (EGFP-GlyT2^{wt}) and both mutants (EGFP-GlyT2$^{\Delta TQC}$, EGFP-GlyT2^{+A}) in order to allow direct visualization by fluorescence microscopy (Fig. 1A). Moreover, we initially used both GlyT2a and b constructs. The encoded proteins differ by only eight amino acids at their N-terminal ends (Ebihara et al., 2004) and showed indistinguishable properties in all our experiments (data not shown). Hence, only the results obtained with the GlyT2a constructs are presented here.

Inactivation of the PDZ-ligand motif does not affect GlyT2 expression and glycosylation

To examine whether the different GlyT2 constructs are expressed at comparable levels, we transiently transfected HEK293T cells with the non-fused wild-type and mutant GlyT2 cDNAs. Detergent
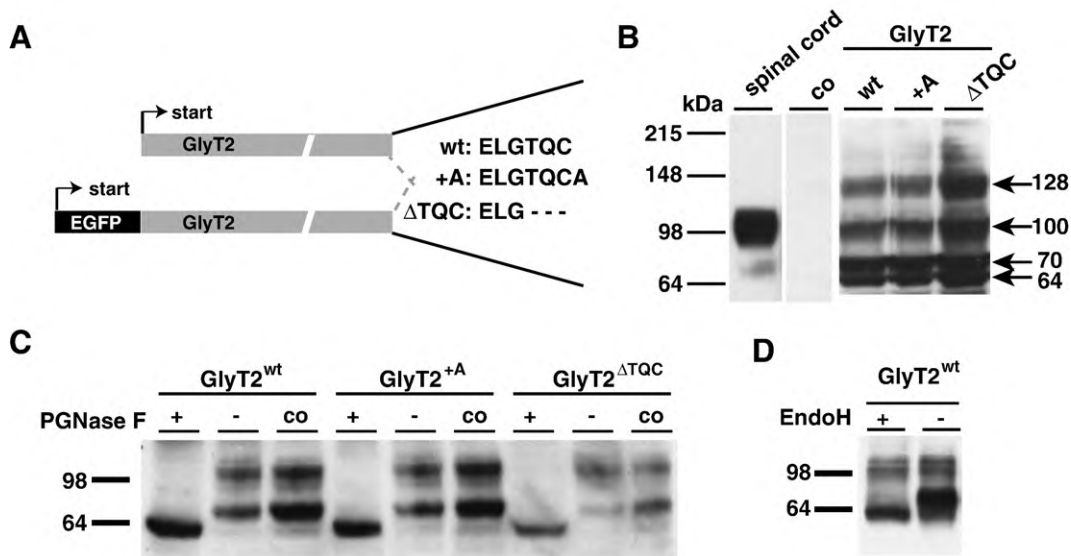

Fig. 1. GlyT2 proteins with inactive PDZ-ligand motif are expressed and glycosylated in HEK293T cells. (A) Design of GlyT2 and EGFP-GlyT2 mutant proteins. For EGFP-GlyT2 fusion proteins, the start ATG codon of the GlyT2 cDNA was removed. The C-terminal amino acid sequences are indicated, including the mutations introduced to inactivate the PDZ-ligand motif. (B) HEK293T cells were transfected with the different GlyT2 constructs, lysed 48 h after transfection, and 30 μg of lysate protein was analyzed by SDS–PAGE and Western blotting using the N-terminal anti-GlyT2 antibody. A lysate prepared from untransfected HEK293T cells served as negative (co), and a crude membrane fraction prepared from mouse spinal cord (20 μg) as positive, controls. (C, D) GlyT2-transfected HEK293T cell lysates (25 μg total protein) were treated with PGNase F (C, (+) incubated with enzyme, (-) incubated without enzyme, (co) kept on ice) or Endo H (D) for 90 min prior to SDS–PAGE and Western blotting. Note respective band shifts upon enzyme treatment.

extracts prepared from the transfected cells were then analyzed by SDS–PAGE and Western blotting with a GlyT2-specific antibody. As controls, a crude membrane fraction (P2 pellet) isolated from mouse spinal cord and an extract prepared from untransfected HEK293T cells were included. In the P2 membrane fraction, a strong immunoreactive band at 100 kDa and a weaker band at 70 kDa were detected (Fig. 1B); this is consistent with previous studies (Zafra et al., 1995a). In contrast, no band was seen in untransfected HEK293T cells. In all extracts prepared from HEK293T cells transfected with GlyT2 expression constructs, several GlyT2 immunoreactive bands were found, including those at 100 kDa and 70 kDa and additional weaker bands at 64 kDa and 128 kDa. The 128-kDa band was only seen at high levels of overexpression (Fig. 1B) and most likely corresponded to SDS-resistant dimers of the 64-kDa or 70-kDa monomers (I. Bartholomaeus and V. Eulenburg, unpublished data). Incubation with PGNase F, a deglycosylating enzyme which removes all sugar side chains, caused a loss of the 100-kDa and the 70-kDa bands, with only the 64-kDa polypeptide remaining, which hence represents the completely deglycosylated GlyT2 protein (Fig. 1C). Upon treatment of the HEK293T cell lysates with Endo H (Fig. 1D), an enzyme, which cleaves only complex mannose residues that are added in the ER (core-glycosylation), the apparent molecular weight of the band at 70 kDa was reduced to 64 kDa, whereas the band at 100 kDa remained unaltered (Fig. 1D). This

indicates that the 70-kDa band represented the core-glycosylated GlyT2 protein. No differences were seen in all these experiments between wild-type and mutant GlyT2 proteins. We therefore conclude that inactivation of the PDZ-ligand motif has no influence on GlyT2 expression and glycosylation.

GlyT2 PDZ-ligand motif mutants are efficiently inserted into and uniformly distributed on the plasma membrane of HEK293T cells

To investigate whether PDZ-ligand motif mutations affect the subcellular localization of GlyT2 in transfected HEK293T cells, we used wild-type and mutant EGFP-GlyT2 fusion proteins for analyzing protein distribution by fluorescence confocal microscopy. In uptake assays and subcellular localization studies with transfected HEK293T cells, these fusion proteins behaved identically to their non-fused counterparts (Supplementary Fig. 1). In contrast to EGFP alone, which was diffusely distributed throughout the cytosol and the nucleus (Supplementary Fig. 1D), the EGFP-GlyT2^{wt} protein showed clear accumulation at the plasma membrane (Fig. 2A). Only weak cytoplasmic fluorescence was detected, which appeared to be associated with the endoplasmic reticulum (ER), as demonstrated by coexpression of an ER-retained Ds-Red-marker (Fig. 2A). A similar partial ER localization has been reported previously for other plasma membrane proteins and has been attributed to overexpression
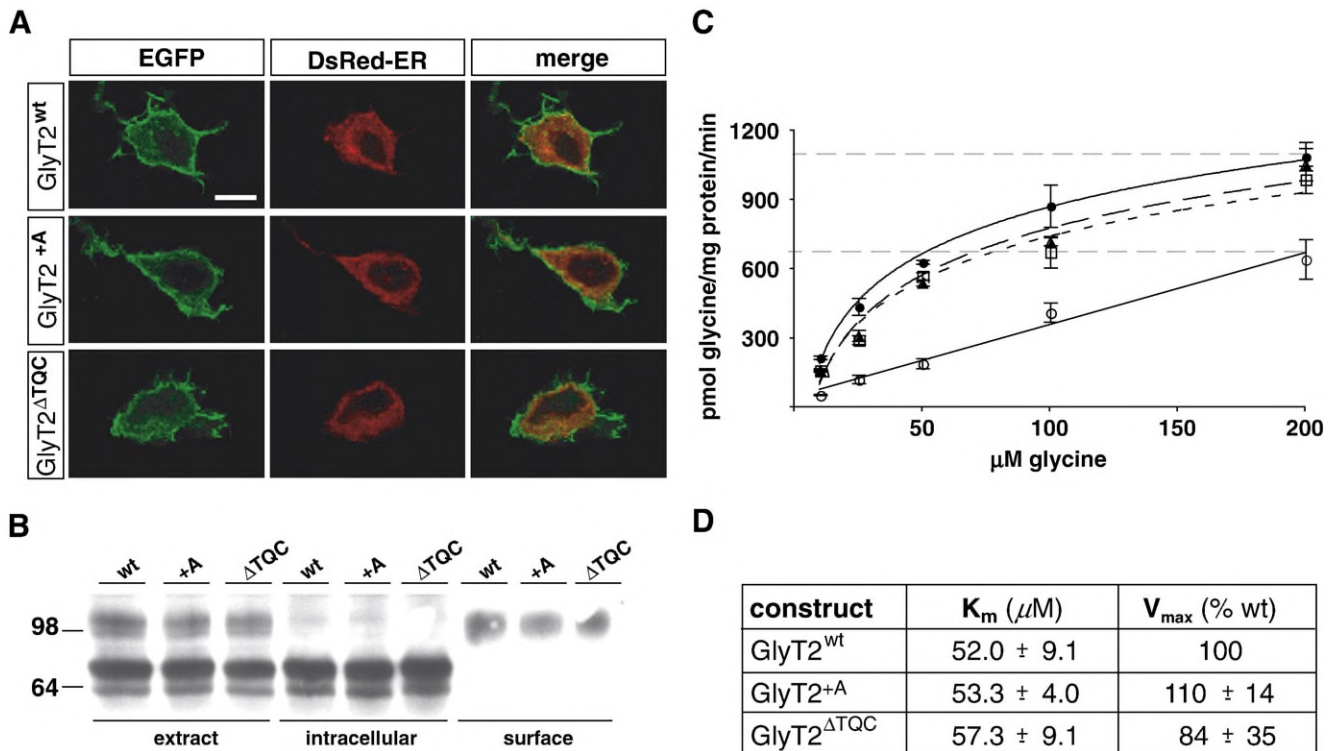

construct	K_m (μM)	V_{max} (% wt)
GlyT2^{wt}	52.0 ± 9.1	100
GlyT2^{+A}	53.3 ± 4.0	110 ± 14
GlyT2$^{\Delta TQC}$	57.3 ± 9.1	84 ± 35

Fig. 2. Surface expression and [^{3}H]glycine uptake are unaltered in PDZ-ligand motif mutants of GlyT2. (A) HEK293T cells were cotransfected 48 h prior to fixation with the indicated EGFP-GlyT2^{wt} or -PDZ-ligand motif mutant cDNAs (green) and pDS-Red-ER (red). Note plasma membrane localization of the EGFP fluorescence; in addition partial colocalization of intracellular fluorescence with the ER marker. Scale bar, 8 μm. (B) With untagged GlyT2 transfected HEK293T cells were surface-biotinylated, and cell extracts fractionated on streptavidin–agarose. Fractions were analyzed by SDS–PAGE and Western blotting with a GlyT2-specific antibody raised against the N-terminal domain of GlyT2. The total extract lanes demonstrate efficient GlyT2 protein expression (extract). The supernatant of the streptavidin–agarose beads, containing proteins not coupled to biotin, represent the intracellular fraction, agarose-bound proteins the surface fraction. (C) HEK293T cells were transfected with pEGFPN1 (open circles, solid line); GlyT2^{wt} (filled circles, solid line); GlyT2^{+A} (triangles, dashed line); GlyT2$^{\Delta TQC}$ (squares, dotted line); and [^{3}H]glycine uptake was determined at room temperature for 4 min. A single representative experiment is shown. (D) Mean K_m and V_{max} values of [^{3}H]glycine uptake ($n=5$). V_{max} values were calculated as percentage of GlyT2^{wt} uptake.

resulting from transient transfection (Schroder and Kaufman, 2005). The localizations of the PDZ-ligand motif mutant proteins were indistinguishable from that of GlyT2[wt]. Also, all EGFP fluorescence appeared to correspond to GlyT2 protein, as staining of the transfected HEK293T cells with a GlyT2-specific antibody resulted in a complete overlap of the EGFP- and GlyT2 immunofluorescences (Supplementary Fig. 1D).

Unimpaired plasma membrane incorporation of the PDZ-ligand motif mutants was confirmed further by surface biotinylation experiments, which allow for a more direct assessment of surface-localized protein. HEK293T cells transfected with the different GlyT2 constructs were treated with sulfo-NHS-SS-biotin, lysed and incubated with streptavidin-coupled agarose beads. Due to the hydrophilic nature of the coupling reagent, only proteins expressed on the cell surface are labeled and isolated by this method (Altin and Pagler, 1995; Shimkus et al., 1985). Western blot analysis of the initial detergent extracts again revealed the mature and core-glycosylated GlyT2 bands at 100 kDa and 70 kDa, and the unglycosylated GlyT2 polypeptide at 64 kDa, respectively (Fig. 2B, extract). In the supernatant of the streptavidin-coupled agarose beads, the intensity of the 100-kDa band was strongly reduced, whereas the core-glycosylated band at 70 kDa and the unglycosylated 64 kDa band were unaltered (Fig. 2B, intracellular). In contrast, in the eluates from the streptavidin–agarose beads, which contained the biotinylated surface fraction, only the 100-kDa band was identified (Fig. 2B, surface). Thus, only the mature, fully glycosylated GlyT2 is inserted into the plasma membrane. This result is in agreement with previous reports showing that only complex glycosylated GlyT2 reaches the cell surface (Martinez-Maza et al., 2001). Densitometric analysis of the different bands confirmed that the 100-kDa GlyT2 protein was detected primarily in the plasma membrane fraction (surface), whereas the partially glycosylated 70 kDa protein was excluded from this fraction and enriched in the supernatant containing the intracellular non-bound proteins (Table 1). Comparison of the mutant GlyT2[+A] and GlyT2[ΔTQC] bands revealed no significant differences to the wild-type protein (Fig. 2B and Table 1). Obviously, inactivation of the PDZ-ligand motif does not affect plasma membrane insertion and surface distribution of GlyT2 in HEK293T cells.

GlyT2 PDZ-ligand motif mutants display transport activity

Deletion or inactivation of the PDZ-ligand motif might alter GlyT2 transport function. We therefore performed [³H]glycine uptake experiments in transfected HEK293T cells 48 h after transfection (Fig. 2C). Variations in transfection efficacy or cell viability were excluded by determining protein expression by both Western blotting and immunocytochemical staining with GlyT2 antibody (data not shown). With all constructs, saturation of [³H] glycine uptake was reached at glycine concentrations of about 150–300 μM. The mean K_m values obtained in five independent experiments were not significantly different between the wild-type and the two mutant proteins (Fig. 2D). The same held true for the respective V_{max} values calculated as percent of wild-type uptake activity. Similar results were also obtained 24 h and 72 h after transfection (not shown), indicating that the number of transporters in the plasma membrane was not changed significantly by PDZ-ligand motif inactivation. In conclusion, these results show that the PDZ-ligand motif of GlyT2 is not essential for substrate transport.

Ectopic expression in hippocampal neurons generates GlyT2 clusters

Although inactivation of the PDZ-ligand motif did not affect GlyT2 expression and function in HEK293T cells, this motif might be important for proper targeting in neurons. For example, the transport machinery or interacting proteins essential for proper GlyT2 localization at inhibitory presynaptic terminals might not be present in HEK293T cells. Hence, we performed transfection experiments with primary neurons, initially using mouse spinal cord cultures prepared at embryonic day 14 (E14). However, in contrast to what is seen with spinal cord sections (data not shown, but see Zafra et al., 1995a), even after 3 weeks in vitro endogenous GlyT2 immunoreactivity was only partially sequestered into punctate structures indicative of presynaptic GlyT2 localization but additionally spread throughout the neurites and somata of presumptive glycinergic neurons (Fig. 3A; see also Poyatos et al., 1997). This presumably reflects the fact that spinal cord cultures have to be prepared at early embryonic stages (E14), whereas the major phase of GlyT2 expression starts only during the first and second postnatal weeks, i.e., at a stage of differentiation that is barely reached under culture conditions.

A recent study has shown that a minor fraction of hippocampal neurons expresses GlyT2 endogenously, which is then targeted to presynaptic sites (Danglot et al., 2004). This indicates that at least a subset of hippocampal neurons contains the trafficking machinery required for proper GlyT2 localization. Therefore, we prepared rat hippocampal neuron cultures at E18.5, transfected these with EGFP-GlyT2 plasmids at day 10 in vitro (DIV10) and fixed 3 days later. EGFP fluorescence of the fusion proteins was hardly detectable at this time point, but staining with GlyT2-specific antibodies revealed a diffuse distribution of EGFP-GlyT2 protein in all neuronal processes. No GlyT2 immunostaining was detected in non-transfected control cultures, indicating that immunofluorescence signals were derived from the EGFP-GlyT2 fusion proteins. In addition, a punctate pattern of EGFP-GlyT2 was observed in most of the neurites present for both the wild-type and the PDZ-ligand motif mutant proteins (Fig. 3B). When quantifying the number of these GlyT2-positive puncta per 50 μm neurite length, all constructs analyzed were found to generate similar densities of GlyT2 puncta (Fig. 3C, EGFP-GlyT2[wt]: 4.9±0.4; EGFP-GlyT2[+A]: 5.0±0.5; EGFP-GlyT2[ΔTQC]: 4.8±0.4 puncta per 50 μm neurite length; n=78–132, each). In addition to these punctate clusters within the neurites, GlyT2 immunoreactivity was also enriched at growth cones (not shown). Together these results indicate that, in hippocampal neurons, recombinant EGFP-GlyT2[wt] displays a similar distribution as reported for endogenous GlyT2 (Danglot et al., 2004).

Table 1
Subcellular distribution of GlyT2 proteins determined by surface biotinylation

Construct	Ratio 100 kDa/70 kDa		
	Extract	Intracellular	Surface
GlyT2[wt]	0.96±0.46	0.15±0.14	12.62±3.96
GlyT2[+A]	0.98±0.58	0.11±0.17	13.65±1.97
GlyT2[ΔTQC]	1.00±0.55	0.10±0.14	13.38±4.70

HEK293T cells transfected with the indicated constructs were surface-biotinylated and fractionated on streptavidin–agarose followed by SDS–PAGE and Western blotting with an antibody raised against the N-terminal domain of GlyT2. GlyT2 immunoreactive bands were quantified densitometrically using NIH Image 1.63. Values represent ratios of the 100-kDa and 70-kDa band intensities (n=4).
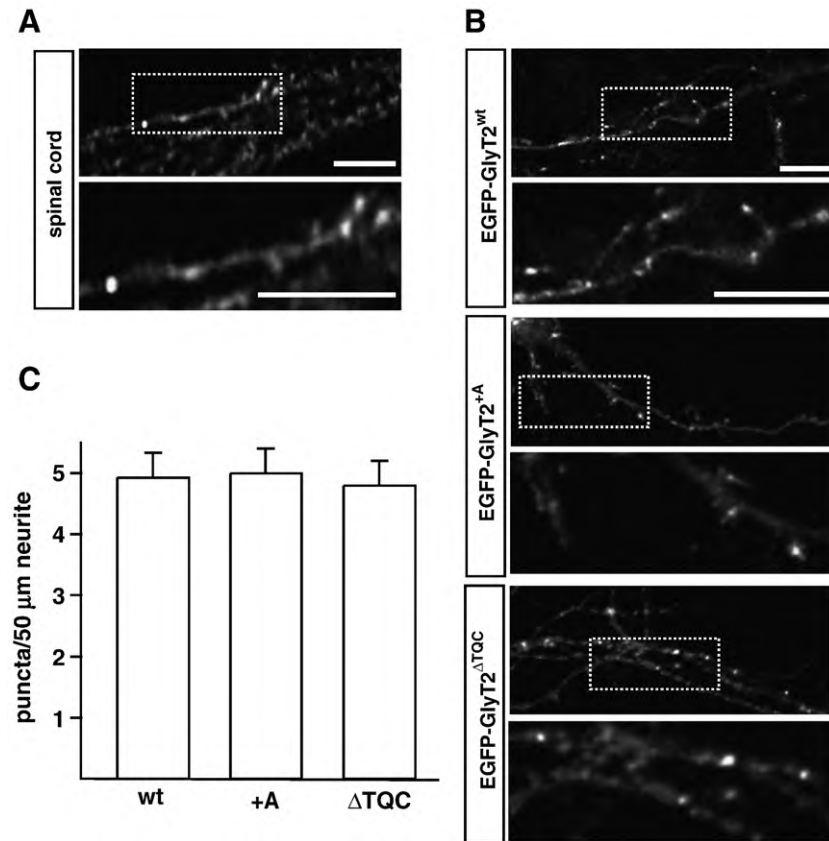
Fig. 3. Recombinant GlyT2 accumulates in punctate structures in transfected hippocampal neurons. (A) Endogenous GlyT2 immunoreactivity revealed with an antibody raised against the C-terminal domain of GlyT2 in cultured spinal cord neurons at DIV14. Note that GlyT2 staining is not restricted to presumptive synaptic sites, but also distributed throughout the neurite. (B) Hippocampal neurons (DIV10) were transfected with either EGFP-GlyT2^{wt} or the indicated EGFP-PDZ-ligand motif mutants. Cells were fixed at DIV13 and stained with a GlyT2-specific antibody raised against the C-terminal domain to increase signal intensity. Besides basal ubiquitous staining of all neurites, GlyT2-immunoreactivity was enriched in punctate structures of the transfected cells. (C) EGFP-GlyT2 puncta densities determined with the different constructs ($n = 78$–132). Scale bars in panels A and B, 8 μm.

The PDZ-ligand motif is important for synaptic localization of GlyT2

To examine whether the punctate EGFP-GlyT2 immunoreactivity described above corresponded to sites of synaptic transporter localization, we performed double-labeling experiments with antibodies specific for the synaptic vesicle protein synaptophysin. After 3 days of recombinant protein expression, $41.0\% \pm 1.2\%$ of the EGFP-GlyT2^{wt} puncta were found to colocalize with synaptophysin immunoreactivity (Fig. 4A). Thus, a substantial fraction of the EGFP-GlyT2^{wt} protein was associated with presynaptic terminals. When parallel cultures expressing the GlyT2 mutants were similarly examined, significantly reduced colocalization values were obtained (EGFP-GlyT2^{+A} $24.7 \pm 2.0\%$, $p < 0.0003$; EGFP-GlyT2$^{\Delta TQC}$ $18.3 \pm 3.0\%$, $p < 0.0003$; $n = 16$–34, each; see Figs. 4A and B). Notably, overall cluster densities were similar with all GlyT2 proteins studied (EGFP-GlyT2^{wt} 5.6 ± 1.3; EGFP-GlyT2^{+A} 5.5 ± 1.3; EGFP-GlyT2$^{\Delta TQC}$ 4.8 ± 1.0 GlyT2 clusters per 50 μm neurite length; n as above). This suggests that the differences in colocalization noted cannot be attributed to different levels of GlyT2 protein expression but result from inactivation of the PDZ-ligand motif. Similar data were obtained in colabeling experiments with antibodies against the synaptic vesicle associated protein VAMP2. Here, $43.3 \pm 0.7\%$ of the EGFP-GlyT2^{wt} clusters colocalized with this synaptic marker,

whereas only $29.1 \pm 1.8\%$ of the EGFP-GlyT2^{+A} ($p < 0.003$) and $25.7 \pm 2.4\%$ of the EGFP-GlyT2$^{\Delta TQC}$ protein showed colocalization with VAMP2 immunoreactivity ($p < 0.0003$; $n = 11$–13, each; see Figs. 4C and D). Again, cluster densities of the ectopically expressed EGFP-GlyT2 proteins were similar, indicating that all three proteins were expressed at comparable levels (EGFP-GlyT2^{wt}: 4.9 ± 0.7; EGFP-GlyT2^{+A}: 4.8 ± 0.5; EGFP-GlyT2$^{\Delta TQC}$ 4.8 ± 0.8 puncta per 50 μm neurite length; $n = 11$–13, each). Taken together, these data indicate that in hippocampal neurons a significant fraction of GlyT2 immunoreactivity is accumulated at synaptic sites, and that this localization is partially dependent on the PDZ-ligand motif.

To examine whether the synaptic GlyT2 clusters seen in hippocampal neurons transfected with the EGFP-GlyT2^{wt}, EGFP-GlyT2^{+A} or EGFP-GlyT2$^{\Delta TQC}$ constructs were associated with inhibitory nerve terminals, we performed double-labeling experiments with antibodies specific for the inhibitory presynaptic marker protein VIAAT (Dumoulin et al., 1999). Consistently, a significant fraction of the EGFP-GlyT2^{wt} puncta was found to colocalize with VIAAT immunoreactivity (Fig. 5A), implying that GlyT2 was indeed presynaptically localized. Qualitatively similar results were obtained with the PDZ-ligand motif mutants (Fig. 5A). Quantification of the number of EGFP-GlyT2 puncta colocalizing with VIAAT revealed, however, that in transfected neurons about $26.0 \pm 2.0\%$ of the EGFP-GlyT2^{wt} clusters were VIAAT-positive whereas a lower
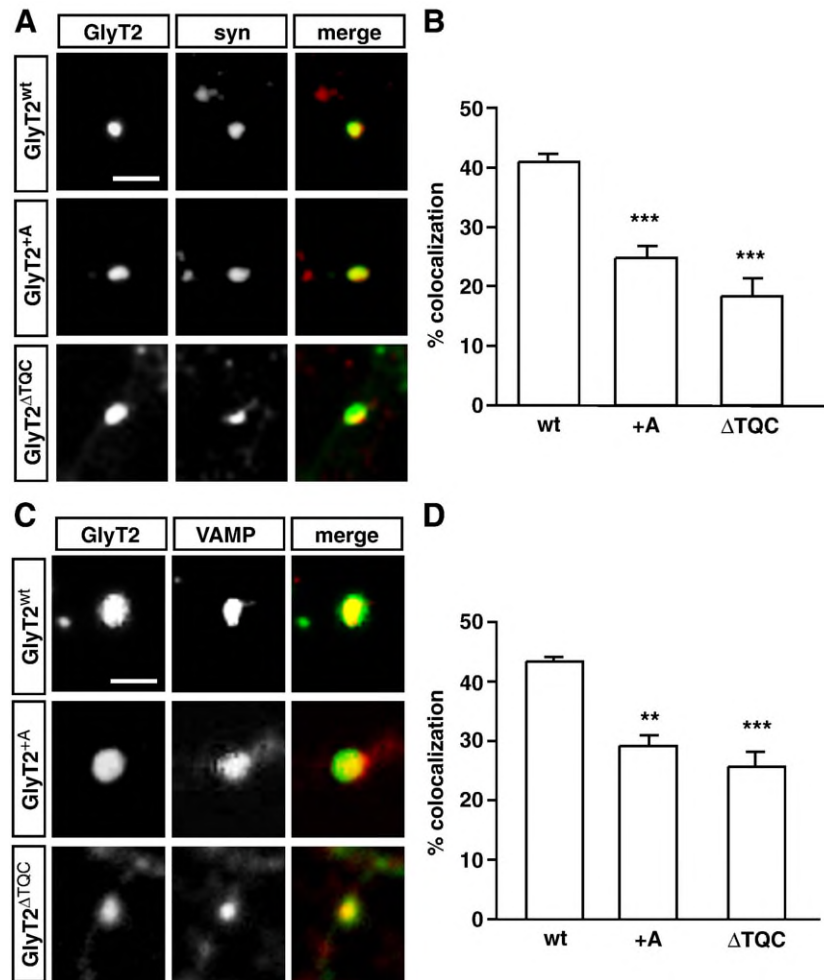
Fig. 4. Recombinant GlyT2 is localized at synaptic sites in transfected hippocampal neurons. Hippocampal neurons were transfected with EGFP-GlyT2^{wt}, EGFP-GlyT2^{+A} or EGFP-GlyT2$^{\Delta TQC}$. Three days after transfection, the cultures were fixed and stained for GlyT2 with the C-terminal antibody (green) and synaptophysin (A), or VAMP2 (C), specific antibodies (red). Note colocalization of GlyT2 staining with these synaptic markers (A, C). Quantification of double immunoreactive puncta for the different GlyT2 constructs and synaptophysin (B, $n=16$–34) and VAMP2 (D, $n=11$–13). Note that inactivation of the PDZ-ligand motif resulted in a reduction of synaptically localized clusters. Significantly different from wt: **$p<0.003$; ***$p<0.0003$. Scale bar panels in A and C, 1 μm.

colocalization value was obtained with the EGFP-GlyT2^{+A} mutant (20.6±2.1%; $p<0.03$). An even more significant reduction in double-positive clusters was found with the deletion mutant EGFP-GlyT2$^{\Delta TQC}$ (11.3±2.8%; $p<0.003$). This corresponds to <50% of the colocalization found with the wild-type protein (Fig. 5B). The overall densities of VIAAT-positive puncta were similar in these experiments with all EGFP-GlyT2 constructs tested although a high variability between different experiments was found (EGFP-GlyT2^{wt}: 3.4±2.5; EGFP-GlyT2^{+A}: 2.5±1.7; EGFP-GlyT2$^{\Delta TQC}$: 2.8±1.9 clusters per 50 μm neurite length, $n=45$, each). Similarly, the density of GlyT2 immunoreactive clusters, which is indicative of GlyT2 expression levels did not differ significantly between the constructs (EGFP-GlyT2^{wt}: 5.6±1.8; EGFP-GlyT2^{+A}: 5.4±1.9; EGFP-GlyT2$^{\Delta TQC}$: 5.1±1.6 clusters per 50 μm neurite length, $n=45$, each).

We also examined GlyT2 colocalization with gephyrin, a scaffolding protein found at both GABAergic and glycinergic postsynapses (Kneussel and Betz, 2000). In contrast to the full colocalization seen with synaptophysin, VAMP2 and VIAAT, gephyrin immunoreactivity was found apposed to GlyT2-positive clusters

(Fig. 5C). This apposition was also observed with both PDZ-ligand motif mutants. Quantification showed that about 40.3±2.2% of all gephyrin puncta were apposed to EGFP-GlyT2^{wt} (Fig. 5D). For the EGFP-GlyT2^{+A} protein, this value was reduced to 30.5±2.1% ($p<0.03$) and for EGFP-GlyT2$^{\Delta TQC}$ to 21.5±2.0% ($p<0.003$), i.e., a ca. 50% reduction as compared to the wild-type protein. Again, the overall cluster densities were similar for wild-type and the mutant proteins (EGFP-GlyT2^{wt}: 5.8±1.9; EGFP-GlyT2^{+A}: 5.5±1.8; EGFP-GlyT2$^{\Delta TQC}$: 5.0±1.9 clusters per 50 μm neurite length; $n=45$, each) as well as for gephyrin (transfected with EGFP-GlyT2^{wt}: 4.2±1.6; EGFP-GlyT2^{+A}: 5.5±1.4; EGFP-GlyT2$^{\Delta TQC}$: 3.4±1.6 gephyrin clusters per 50 μm neurite-length, $n=45$; each). In summary, upon inactivation of the PDZ-ligand motif the percentage of GlyT2 clusters associated with inhibitory synapse markers was reduced by 20–30% and 45–55%, respectively.

To analyze whether the VIAAT clusters represent inhibitory synaptic specializations, we investigated the colocalization of gephyrin and VIAAT in our hippocampal cultures. Consistent with the literature (Danglot et al., 2003), we found that 88±2% of the gephyrin clusters colocalized with VIAAT immunoreactivity,
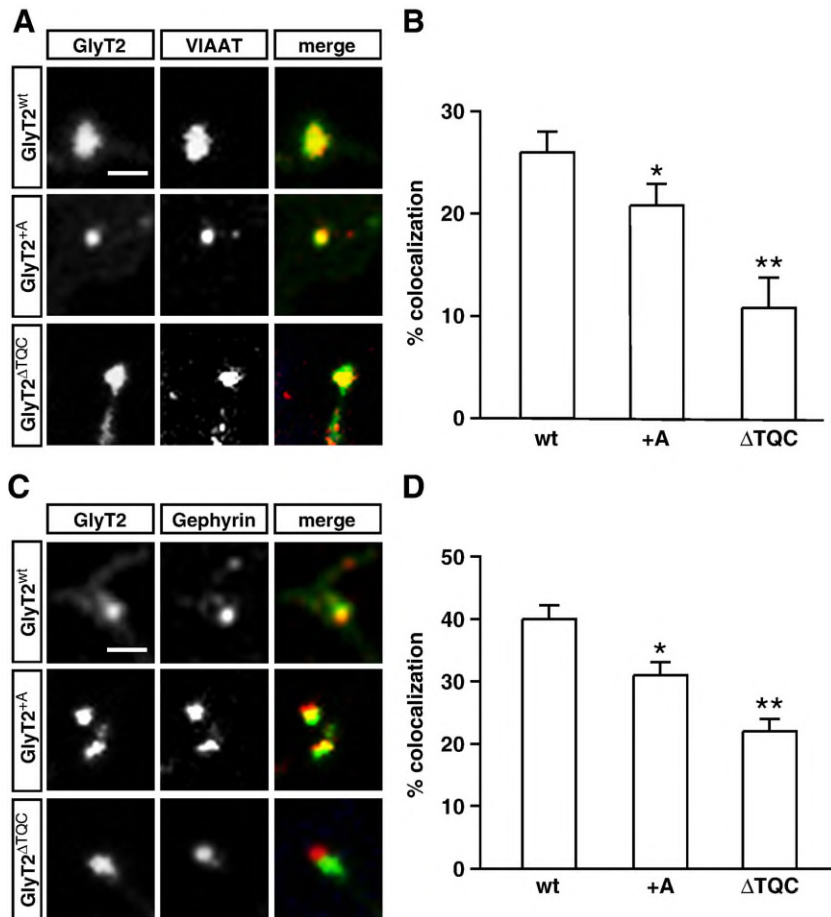
Fig. 5. Reduced localization of GlyT2 PDZ-ligand motif mutants at inhibitory synapses. Hippocampal neurons transfected with EGFP-GlyT2^{wt} or the indicated PDZ-ligand motif mutants were stained for GlyT2 (green) with the C-terminal anti-GlyT2 antibody and the inhibitory synaptic marker proteins VIAAT (red, A) or gephyrin (red, C). Note that full colocalization only occurred with presynaptically localized VIAAT, whereas the postsynaptic marker protein gephyrin was only apposed (B, D). Colocalization of GlyT2 with VIAAT (B), or gephyrin (D), at double immuno-positive puncta ($n=45$, each). Significantly different from wt: $*p \leq 0.03$; $**p \leq 0.003$. Scale bar in panels A and C, 1 μm.

indicating that most VIAAT positive structures were associated with inhibitory postsynaptic membrane specializations (data not shown). In addition, no differences were observed between neurons transfected with the different EGFP-GlyT2 constructs (gephyrin/VIAAT colocalization in cells transfected with EGFP-GlyT2^{wt}: 87.1%±0.9; in EGFP-GlyT2^{+A}: 87.9%±1.1; in EGFP-GlyT2$^{\Delta TQC}$: 89.0%±1.2; $n=45$, each).

In hippocampal cultures, the majority of the neurons are excitatory and therefore do not express VIAAT (Chaudhry et al., 1998; Liu, 2004). Thus, transfection of these cells cannot result in colocalization with presynaptic marker proteins of inhibitory synapses. To examine whether GlyT2 clusters, negative for VIAAT or gephyrin, might be localized at excitatory synapses, we performed double immunolabeling for GlyT2 and the postsynaptic density protein PSD95. This revealed consistent apposition of the two immunoreactivities at several sites (Fig. 6A). Quantitative evaluation showed that about 26.0±1.6% of the PSD95-positive clusters analyzed ($n=134$) contained EGFP-GlyT2^{wt} in the transfected neurons (Fig. 6B). An average of 10.0±4.2 PSD95-puncta and of 4.9±2.0 EGFP-GlyT2^{wt} puncta were counted per 50 μm neurite length. For EGFP-GlyT2$^{\Delta TQC}$ and EGFP-GlyT2^{+A}, overall density numbers were similar (GlyT2$^{\Delta TQC}$: 4.2±2.1, GlyT2^{+A}: 5.0±2.5

clusters per 50 μm neurite length; $n=78$–128, each), as were the numbers of PSD95 clusters (EGFP-GlyT2^{wt}: 10.0±4.2; EGFP-GlyT2^{+A}: 11.1±5.5; EGFP-GlyT2$^{\Delta TQC}$: 9.5±4.0 clusters per 50 μm neurite length; $n=78$–134, each). In contrast, colocalization with PSD95 was reduced by >50% for both PDZ-ligand motif mutants as compared to wild-type (EGFP-GlyT2^{wt}: 26.0±0.6%; EGFP-GlyT2$^{\Delta TQC}$: 11.8±0.6% ($p<0.0003$); EGFP-GlyT2^{+A} 10.2±0.6% ($p<0.0003$).

These results were further confirmed by colabeling experiments using the presynaptically localized vesicular glutamate transporter VGLUT2. In these experiments, EGFP-GlyT2^{wt} showed 43.6± 1.4% colocalization with VGLUT2. Similar to our results with PSD95, stainings of EGFP-GlyT2^{+A} and EGFP-GlyT2$^{\Delta TQC}$ resulted in a markedly reduced colocalization. Here, only 30.7±1.8% for EGFP-GlyT2^{+A} ($p<0.003$) and 22.5±3.1% ($p<0.0003$) of the EGFP-GlyT2$^{\Delta TQC}$ clusters colocalized with VGLUT2, although VGLUT2-cluster (EGFP-GlyT2^{wt}: 6±0.9; EGFP-GlyT2^{+A}: 6±0.6, EGFP-GlyT2$^{\Delta TQC}$ 6.2±0.9) and GlyT2-cluster densities (EGFP-GlyT2^{wt} 4.7±0.7, EGFP-GlyT2^{+A}: 4.6±0.6, EGFP-GlyT2$^{\Delta TQC}$ 5± 0.8 clusters per 50 μm neurite length, $n=13$–24, each) were similar in all three cultures. Thus, the ectopic expression of GlyT2 in excitatory neurons results in an accumulation of GlyT2 at excitatory
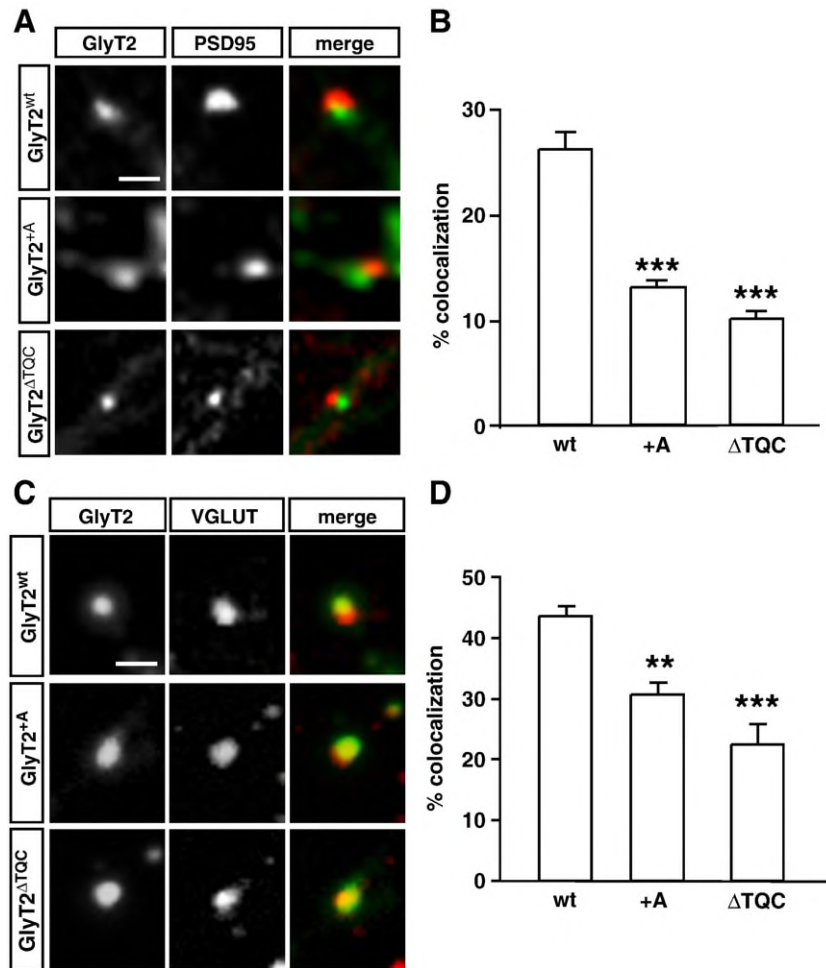
Fig. 6. Reduced synaptic localization of GlyT2 PDZ-ligand motif mutants at excitatory synapses. Hippocampal neurons transfected with EGFP-GlyT2[wt] or the indicated PDZ-ligand motif mutants were stained for GlyT2 (green) with the C-terminal antibody and PSD95 (red, A) or VGLUT2 (red, C). Note that GlyT2 and PSD95 immunoreactivities are not fully colocalized but appositioned. (B, D) Quantification of GlyT2 and PSD95 (B), or VGLUT2 (D), colocalization at double-immunopositive puncta ($n = 78–134$ for (B), and $n = 13–24$ for (D), respectively). Significantly different from wt: $**p < 0.003$; $***p < 0.0003$. Scale bar, 1 µm.

synaptic sites. Together these data show that both inactivation and deletion of the PDZ-ligand motif of GlyT2 reduces the synaptic localization of this transporter.

Discussion

In this study, we investigated possible functions of the PDZ-ligand motif of GlyT2 in the processing, surface delivery, trafficking and synaptic targeting of this membrane protein in both HEK293T cells and primary hippocampal neurons by a loss-of-function approach. PDZ-ligand motif inactivation had no effect on transporter expression, plasma membrane insertion and function in HEK293T cells. In primary hippocampal neurons, however, mutation of the PDZ-ligand motif resulted in a significant reduction of GlyT2 synaptic localization, suggesting that this motif is required for efficient sequestering of the transporter to synaptic sites.

In a previous study, we have identified syntenin-1 as an interaction partner of GlyT2 (Ohno et al., 2004). Syntenin-1 is a protein containing two PDZ domains, which both contribute to binding to GlyT2 and interact with the non-classical class III PDZ-ligand motif located at the extreme C-terminus of this transporter.

Sequence comparisons and yeast two-hybrid studies have disclosed PDZ-ligand motifs at the extreme C-termini of most family members of the *SLC6a* family, including the GlyT1, dopamine transporter, DAT, and the GABA transporters GAT1-3 (Brown et al., 2004; Cubelos et al., 2005b; Muth et al., 1998; Torres et al., 2001). A more detailed analysis of the precise functions of these motifs has been constrained by the presence of other regulatory domains within the C-terminal cytoplasmic tails of these proteins that lie in close proximity to the PDZ-ligand motif. Within DAT and GAT1, such elements have been shown to be essential for ER export (Bjerggaard et al., 2004; Farhan et al., 2004).

Here, we disrupted the PDZ-ligand motif of GlyT2 by truncation of the three C-terminal amino acids (GlyT2[ΔTQC]) or by masking the carboxyterminus via addition of an alanine residue (GlyT2[+A]). Both mutations have been previously shown to cause PDZ-ligand motif inactivation, and to thereby inhibit binding of syntenin-1 to the C-terminus of GlyT2 (Ohno et al., 2004). Analysis of transfected HEK293T cells revealed that both the wild-type and mutant GlyT2 proteins were expressed at similar levels and indistinguishable in glycosylation, subcellular localization and transport activity. Hence, the PDZ-ligand motif is not essential for transporter folding, ER

export or membrane insertion in this mammalian cell line. Our result contrasts a report in which inactivation of the C-terminal PDZ-ligand motif of the DAT has been found to decrease uptake activity, most likely due to enhanced internalization (Torres et al., 2001). Further evidence for a role of the PDZ-ligand motif in the regulation of neurotransmitter uptake comes from studies on GlyT1 and DAT. Here, coexpression of proteins interacting with these transporters via their PDZ-ligand motif (PSD95 for GlyT1, and PICK1 for DAT, respectively) resulted in transporter stabilization at the cell surface, and thereby increased transport activity (Cubelos et al., 2005b; Torres et al., 2001). In similar experiments, coexpression of syntenin-1 failed to increase GlyT2-mediated glycine uptake into HEK293T cells (Ohno et al., 2004). Thus, PDZ-ligand motifs may have distinct functions in different transporter proteins.

Comparison of the localization of the endogenously expressed GlyT2 protein in dissociated spinal neurons with ectopically expressed GlyT2^{wt} in hippocampal neurons revealed similar distributions of GlyT2 immunoreactivity in both cell systems. Further immunocytochemical analysis using antibodies specific for the presynaptic marker proteins synaptophysin and VAMP2 confirmed that GlyT2 is partially enriched at synaptic sites in hippocampal neurons, showing that these cells contain the components required for synaptic trafficking of the transporter. Colocalization with the inhibitory synapse markers VIAAT and gephyrin revealed that a subset of the GlyT2 clusters is localized at inhibitory synaptic sites. This is consistent with a previous report, which demonstrated a synaptic localization of endogenously expressed GlyT2 within a subset of hippocampal neurons (Danglot et al., 2004). The large fraction of GlyT2 clusters that did not colocalize with VIAAT and gephyrin presumably reflects the relatively low percentage of inhibitory neurons present in our hippocampal cultures (<20%, Boehm and Betz, 1997). Consistent with this explanation, GlyT2 was also enriched at presynaptic sites of excitatory neurons, as revealed by colocalization with VGLUT2 and apposition to the postsynaptic marker protein PSD95. Thus, both inhibitory and excitatory neurons in this culture system seem to have the capacity to cluster GlyT2 at synapses.

The synaptic enrichment of exogenously expressed GlyT2 seen here in hippocampal neurons contrasts previously published results (Poyatos et al., 2000). There, GlyT2 was distributed uniformly over the neuronal plasma membrane upon viral overexpression. We attribute this difference to the high expression levels and rapid time course of expression achieved under these conditions. Indeed, we also saw a uniform plasma membrane fluorescence when analyzing neurons transfected with the EGFP-GlyT2 construct for less than 24 h (data not shown). Longer expression times (48–96 h), however, did not only lead to a loss of overexpressing cells, but also to an accumulation of punctate GlyT2 immunoreactivity in the transfected neurons. Thus, the transport of GlyT2 protein to presynaptic sites appears to be a relatively slow process.

Inactivation of the PDZ-ligand motif decreased the number of GlyT2 puncta colocalizing with synaptic markers. This indicates that this motif is important for synaptic localization but dispensable for the clustering of GlyT2 in hippocampal neurons. Synaptic recruitment of GlyT2 might be mediated by its binding to syntenin-1. This hypothesis is supported by studies suggesting that syntenin-1 is involved in presynaptic membrane differentiation during the neuronal development (Hirbec et al., 2005). Specifically syntenin-1 has been shown to be clustered at excitatory presynaptic release sites via the presynaptic protein ERC/CAST1. Although respective experimental data are lacking, similar

syntenin-1 clusters have been proposed to exist at inhibitory synapses (Ko et al., 2006). A role of PDZ-ligand motifs in presynaptic clustering and/or targeting has been demonstrated for metabotropic glutamate receptor 7 (mGluR7) and DAT, two proteins that interact with PICK1 (Stowell and Craig, 1999; Torres et al., 2001). In mGluR7, the C-terminal PDZ-ligand motif was found to be required for presynaptic enrichment but not axonal targeting of this receptor (Boudin et al., 2000). Since the complete C-terminal cytoplasmic tail sequence has been reported to be necessary and sufficient for axonal targeting of mGluR7 (Stowell and Craig, 1999), additional targeting motifs must exist within this region of the receptor. In the case of DAT, inactivation of the PDZ-ligand motif seems not only to cause a loss of the transporter from synaptic sites but to prevent it from entering the axonal compartment (Torres et al., 2001). The precise molecular mechanisms underlying axonal targeting and synaptic recruitment are still not understood. Thus, it remains unclear whether inactivation of the PDZ-ligand motif results in reduced protein delivery to synaptic sites or increased internalization and/or degradation of the synaptically localized membrane proteins.

Although both GlyT2 PDZ-ligand motif mutants analyzed here displayed a reduction in synaptically localized clusters, the extent of reduction differed between the two mutants. At inhibitory synapses, the GlyT2^{+A} mutant showed only a modestly reduced colocalization with the marker proteins VIAAT and gephyrin as compared to the wild-type transporter, whereas truncation of the last three amino acids produced a more drastic reduction in synaptic enrichment. This might indicate that in addition to PDZ domain-mediated interactions with proteins like syntenin-1, additional binding motifs located in proximity to the PDZ-ligand motif contribute to the recruitment and/or stabilization of GlyT2 at inhibitory synapses. Such a motif has been identified within the C-terminus of the DAT, and its disruption has been found to result in intracellular retention of the transporter (Bjerggaard et al., 2004). In contrast, in excitatory neurons the apposition of the GlyT2^{+A} mutant to PSD-95 was as efficiently reduced as that of the GlyT2^{ΔTQC} protein. This suggests that the PDZ-ligand interactions contributing to the presynaptic accumulation of the GlyT2 may involve different interacting proteins in excitatory as compared to inhibitory neurons.

In conclusion, our results show that the C-terminal intracellular domain of GlyT2 is important for synaptic localization of this transporter. Comparison of the two mutants analyzed in this study suggests that the presynaptic enrichment of this transporter depends on its PDZ-ligand motif. In addition, yet undefined determinants of synaptic targeting seem to be present within the C-terminus of GlyT2. Future work should reveal whether PDZ-ligand motif deficient transporters are inefficiently recruited to or poorly stabilized at synaptic sites.

Experimental methods

Materials

The following antibodies were used for immunocytochemistry and/or Western blotting: polyclonal GlyT2-specific antibodies, raised against the C-terminal domain (Guinea pig, Chemicon Temecula, USA, 1:5000, used for staining of neuronal cultures) or the N-terminal domain (Gomeza et al., 2003b, 1:500–1:2000); anti-EGFP (mouse monoclonal, clone Jl-8; Clontech, Mountain View, USA); anti-VIAAT (rabbit polyclonal, kindly provided by Bruno Gasnier, 1:1000); anti-gephyrin (mouse, monoclonal; mab7, Pfeiffer et al., 1984, 1:200); anti-synaptophysin (mouse monoclonal, SVP38, Sigma, St. Louis, USA 1:100–1:200, clone MAB368, Chemicon, 1:200); anti-VGLUT2

(rabbit polyclonal, 1:250–1:400); anti-VAMP2 (mouse monoclonal, 1:1200, both from Synaptic Systems, Goettingen, Germany); and anti-PSD95 (mouse monoclonal, 1:25, Chemicon). Secondary antibodies (guinea pig, rabbit or mouse, Alexa-488, Alexa-546 or Alexa-635 conjugated for immunocytochemistry, or horseradish peroxidase-conjugated for Western blotting) were from Invitrogen (Karlsruhe, Germany) or Promega (Madison, USA), respectively. [³H]Glycine was purchased from Movarek Biochemicals (Brea, USA), and sulfo-NHS-SS-biotin and streptavidin–agarose from Perbio Science (Bonn, Germany).

Plasmids

The different mouse GlyT2 cDNAs were amplified by PCR from brain stem C57BL6/J cDNA. A *Hin*dIII site and an optimized Kozak sequence were introduced at the 5′ region in front of the start ATG by PCR. The respective C-terminal mutations and an *Eco*RI site were also generated by PCR-based mutagenesis. The cDNA fragments were subcloned into the pcDNA3.1(+) vector (Invitrogen, Carlsbad, USA), using restriction sites *Hin*dIII and *Eco*RI. For subcloning into the pEGFP-C3 vector (Clontech, Mountain View, USA), the start-ATG at the 5′-end was removed and an *Xho*I site was attached to the 5′-region by PCR. The fragment was then ligated via the *Xho*I and *Eco*RI sites of the vector, fusing the GlyT2 sequence in frame to the 3′ end of the EGFP coding region of the vector. The pDsRed2-ER plasmid (Clontech, Mountain View, USA) was used for cotransfection in human embryonic kidney 293T (HEK293T) cells in order to visualize ER membranes.

Culture and transfection of mammalian cells

HEK293T were grown in MEM supplemented with 10% (v/v) heat-inactivated fetal calf serum, 2 mM L-glutamine and antibiotics (all Gibco, Bethesda Research Laboratories, Karlsruhe, Germany) on 10-cm diameter cell culture dishes or on poly-D-lysine-coated glass coverslips at 37 °C in an atmosphere containing 5% CO_2. Cells were transfected (1 µg of DNA per cover slip, or 20 µg per 10 cm dish) by calcium phosphate coprecipitation for 6 h, as described previously (Chen and Okayama, 1987). After transfection, HEK293T cells were cultured for 48 h prior to fixation and immunostaining.

Hippocampal neurons were isolated from E18.5 rat embryos and cultured in 24-well dishes on glass cover slips as described (Fuhrmann et al., 2002). At DIV10, neurons were transfected with Lipofectamine 2000 (Invitrogen, San Diego, USA), using a protocol modified from Jaskolski et al. (2005). In brief, transfection medium (T_0: neurobasal medium with 33 mM glucose) was preincubated for 1 h at 37 °C in an atmosphere containing 5% CO_2 prior to mixing 125 µl T_0 with 2.5 µl Lipofectamine 2000. In a second vial, 1.25 µg DNA were mixed with 125 µl T_0. After a 10-min incubation, the T_0-lipofectamine mix was added to the T_0-DNA mixture and incubated for an additional 10 min. Then the medium was removed from the cells, collected, and replaced by 500 µl T_0, and 50 to 100 µl of the transfection mix were added to each well. The cells were incubated for 45 min at 37 °C in 5% CO_2. The transfection medium was removed, the cells washed twice with T_0 medium and then the previously collected medium was readded to the neurons. The neurons were fixed at DIV13.

Immunostaining and quantification of colocalization

The medium from the transfected cells was aspirated, and the cells were washed with PBS on ice. After fixation (4% (w/v) paraformaldehyde in phosphate-buffered saline (PBS) on ice for 7 min), the cells were washed three times with PBS, incubated for 1 h with blocking solution (2% (v/v) goat serum and 1% (w/v) bovine serum albumin in PBS) followed by a 15-min incubation in blocking solution containing 0.1% (v/v) Triton X-100. The cells were then incubated with primary antibodies diluted in blocking solution for 90 min at RT or over night at 4 °C. After washing three times with PBS for 7 min each, the cells were incubated with Alexa-conjugated secondary antibodies for 30 min prior to washing and mounting in Aquamount (Polyscience Inc., Warrington, USA).

Images were collected at a magnification of 630× on a Leica TSC-SP confocal scanning microscope (Leica Microsystems, Bensheim, Germany) or a Zeiss Axio Imager, equipped with an Apotome (Carl Zeiss, Goettingen, Germany). For quantifying punctate immunofluorescence in hippocampal neurons, images were processed identically with the Metamorph v6.1 program package (Molecular Devices, Sunnyvale, USA). Images containing neurites from more than 10 neurons each derived from at least three distinct preparations but identically processed cultures were captured. The number of GlyT2 puncta and costained clusters of synaptic marker protein (>0.5 µm) was counted per 50 µm of neurite length, and the fraction of puncta showing colocalization determined. Values are expressed as mean±SEM per 50 µm neurite length.

Western blotting and deglycosylation

HEK293T cells were lysed 48 h after transfection in 50 mM HEPES–Tris pH 7.4, containing 150 mM NaCl, 5 mM EDTA, 1% (v/v) Triton X-100, 0.25% (w/v) deoxycholate, 0.1% (w/v) SDS and protease inhibitor cocktail (Roche, Heidelberg, Germany). For deglycosylation experiments with PGNase F or Endo H (both New England Biolabs, Beverly, USA), 30 µg protein was treated with 500 units of the respective enzyme for 90 min at 37 °C. The reaction was stopped with 4× sample buffer and analyzed by SDS–PAGE and Western blotting as described (Eulenburg et al., 2006).

Biotinylation experiments

Surface biotinylation of transfected HEK-293T cells with 1 mM NHS-SS-biotin (Perbio Science) was performed essentially as described (Eulenburg et al., 2006). Unspecifically bound biotin was quenched with 100 mM glycine/PBS. After biotinylation, 50 µl (2 µg/µl) protein lysate were incubated with 50 µl streptavidin–agarose beads (Perbio Science) for 3 h at 4 °C on a shaker. The beads were collected, and the supernatant containing the unbound intracellular protein saved. After washing three times with PBS, bound proteins were eluted using 60 µl 2× sample buffer containing 100 mM DTT for 30 min at room temperature. Lysates, supernatants and proteins eluted from the agarose beads were analyzed by SDS–PAGE and Western blotting.

[³H]Glycine uptake experiments

[³H]Glycine uptake into transfected HEK293T cells was determined as described (Eulenburg et al., 2006).

Appendix A. Supplementary data

Supplementary data associated with this article can be found, in the online version, at doi:10.1016/j.mcn.2007.07.011.

References

Adams, R.H., Sato, K., Shimada, S., Tohyama, M., Puschel, A.W., Betz, H., 1995. Gene structure and glial expression of the glycine transporter GlyT1 in embryonic and adult rodents. J. Neurosci. 15, 2524–2532.

Altin, J.G., Pagler, E.B., 1995. A one-step procedure for biotinylation and chemical cross-linking of lymphocyte surface and intracellular membrane-associated molecules. Anal. Biochem. 224, 382–389.

Betz, H., Laube, B., 2006. Glycine receptors: recent insights into their structural organization and functional diversity. J. Neurochem. 97, 1600–1610.

Bezprozvanny, I., Maximov, A., 2001. PDZ domains: More than just a glue. Proc. Natl. Acad. Sci. U. S. A. 98, 787–789.

Bjerggaard, C., Fog, J.U., Hastrup, H., Madsen, K., Loland, C.J., Javitch, J.A., Gether, U., 2004. Surface targeting of the dopamine transporter involves discrete epitopes in the distal C terminus but does not require canonical PDZ domain interactions. J. Neurosci. 24, 7024–7036.

Boehm, S., Betz, H., 1997. Somatostatin inhibits excitatory transmission at rat hippocampal synapses via presynaptic receptors. J. Neurosci. 17, 4066–4075.

Boudin, H., Doan, A., Xia, J., Shigemoto, R., Huganir, R.L., Worley, P., Craig, A.M., 2000. Presynaptic clustering of mGluR7a requires the PICK1 PDZ domain binding site. Neuron 28, 485–497.

Brown, A., Muth, T., Caplan, M., 2004. The COOH-terminal tail of the GAT-2 GABA transporter contains a novel motif that plays a role in basolateral targeting. Am. J. Physiol., Cell Physiol. 286, C1071–C1077.

Chaudhry, F.A., Reimer, R.J., Bellocchio, E.E., Danbolt, N.C., Osen, K.K., Edwards, R.H., Storm-Mathisen, J., 1998. The vesicular GABA transporter, VGAT, localizes to synaptic vesicles in sets of glycinergic as well as GABAergic neurons. J. Neurosci. 18, 9733–9750.

Chen, C., Okayama, H., 1987. High-efficiency transformation of mammalian cells by plasmid DNA. Mol. Cell. Biol. 7, 2745–2752.

Cubelos, B., Gimenez, C., Zafra, F., 2005a. Localization of the GLYT1 Glycine Transporter at Glutamatergic Synapses in the Rat Brain. Cereb. Cortex 15, 448–459.

Cubelos, B., Gonzalez-Gonzalez, I.M., Gimenez, C., Zafra, F., 2005b. The scaffolding protein PSD-95 interacts with the glycine transporter GLYT1 and impairs its internalization. J. Neurochem. 95, 1047–1058.

Danglot, L., Triller, A., Bessis, A., 2003. Association of gephyrin with synaptic and extrasynaptic GABAA receptors varies during development in cultured hippocampal neurons. Mol. Cell. Neurosci. 23, 264–278.

Danglot, L., Rostaing, P., Triller, A., Bessis, A., 2004. Morphologically identified glycinergic synapses in the hippocampus. Mol. Cell. Neurosci. 27, 394–403.

Dumoulin, A., Rostaing, P., Bedet, C., Levi, S., Isambert, M.F., Henry, J.P., Triller, A., Gasnier, B., 1999. Presence of the vesicular inhibitory amino acid transporter in GABAergic and glycinergic synaptic terminal boutons. J. Cell Sci. 112 (Pt 6), 811–823.

Ebihara, S., Yamamoto, T., Obata, K., Yanagawa, Y., 2004. Gene structure and alternative splicing of the mouse glycine transporter type-2. Biochem. Biophys. Res. Commun. 317, 857–864.

Eulenburg, V., Armsen, W., Betz, H., Gomeza, J., 2005. Glycine transporters: essential regulators of neurotransmission. Trends Biochem. Sci. 30, 325–333.

Eulenburg, V., Becker, K., Gomeza, J., Schmitt, B., Becker, C.M., Betz, H., 2006. Mutations within the human GLYT2 (SLC6A5) gene associated with hyperekplexia. Biochem. Biophys. Res. Commun. 348, 400–405.

Farhan, H., Korkhov, V.M., Paulitschke, V., Dorostkar, M.M., Scholze, P., Kudlacek, O., Freissmuth, M., Sitte, H.H., 2004. Two discontinuous segments in the carboxyl terminus are required for membrane targeting of the rat gamma-aminobutyric acid transporter-1 (GAT1). J. Biol. Chem. 279, 28553–28563.

Fornes, A., Nunez, E., Aragon, C., Lopez-Corcuera, B., 2004. The second intracellular loop of the glycine transporter 2 contains crucial residues for glycine transport and phorbol ester-induced regulation. J. Biol. Chem. 279, 22934–22943.

Fuhrmann, J.C., Kins, S., Rostaing, P., El Far, O., Kirsch, J., Sheng, M., Triller, A., Betz, H., Kneussel, M., 2002. Gephyrin interacts with Dynein light chains 1 and 2, components of motor protein complexes. J. Neurosci. 22, 5393–5402.

Gabernet, L., Pauly-Evers, M., Schwerdel, C., Lentz, M., Bluethmann, H., Vogt, K., Alberati, D., Mohler, H., Boison, D., 2005. Enhancement of the NMDA receptor function by reduction of glycine transporter-1 expression. Neurosci. Lett. 373, 79–84.

Geerlings, A., Lopez-Corcuera, B., Aragon, C., 2000. Characterization of the interactions between the glycine transporters GLYT1 and GLYT2 and the SNARE protein syntaxin 1A. FEBS Lett. 470, 51–54.

Geerlings, A., Nunez, E., Rodenstein, L., Lopez-Corcuera, B., Aragon, C., 2002. Glycine transporter isoforms show differential subcellular localization in PC12 cells. J. Neurochem. 82, 58–65.

Gether, U., Andersen, P.H., Larsson, O.M., Schousboe, A., 2006. Neurotransmitter transporters: molecular function of important drug targets. Trends Pharmacol. Sci. 27, 375–383.

Gomeza, J., Zafra, F., Olivares, L., Gimenez, C., Aragon, C., 1995. Regulation by phorbol esters of the glycine transporter (GLYT1) in glioblastoma cells. Biochim. Biophys. Acta 1233, 41–46.

Gomeza, J., Hulsmann, S., Ohno, K., Eulenburg, V., Szoke, K., Richter, D., Betz, H., 2003a. Inactivation of the glycine transporter 1 gene discloses vital role of glial glycine uptake in glycinergic inhibition. Neuron 40, 785–796.

Gomeza, J., Ohno, K., Hulsmann, S., Armsen, W., Eulenburg, V., Richter, D.W., Laube, B., Betz, H., 2003b. Deletion of the mouse glycine transporter 2 results in a hyperekplexia phenotype and postnatal lethality. Neuron 40, 797–806.

Hirbec, H., Martin, S., Henley, J.M., 2005. Syntenin is involved in the developmental regulation of neuronal membrane architecture. Mol. Cell. Neurosci. 28, 737–746.

Horiuchi, M., El Far, O., Betz, H., 2000. Ulip6, a novel unc-33 and dihydropyrimidinase related protein highly expressed in developing rat brain. FEBS Lett. 480, 283–286.

Horiuchi, M., Loebrich, S., Brandstaetter, J.H., Kneussel, M., Betz, H., 2005. Cellular localization and subcellular distribution of Unc-33-like protein 6, a brain-specific protein of the collapsin response mediator protein family that interacts with the neuronal glycine transporter 2. J. Neurochem. 94, 307–315.

Jaskolski, F., Normand, E., Mulle, C., Coussen, F., 2005. Differential trafficking of GluR7 kainate receptor subunit splice variants. J. Biol. Chem. 280, 22968–22976.

Kim, E., Sheng, M., 2004. PDZ domain proteins of synapses. Nat. Rev., Neurosci. 5, 771–781.

Kneussel, M., Betz, H., 2000. Clustering of inhibitory neurotransmitter receptors at developing postsynaptic sites: the membrane activation model. Trends Neurosci. 23, 429–435.

Ko, J., Yoon, C., Piccoli, G., Kim, K., Lee, J.R., Lee, H.W., Kim, H., Sala, C., Kim, E., 2006. Organization of the presynaptic active zone by ERC2/CAST1-dependent clustering of the tandem PDZ protein syntenin-1. J. Neurosci. 26, 963–970.

Liu, G., 2004. Local structural balance and functional interaction of excitatory and inhibitory synapses in hippocampal dendrites. Nat. Neurosci. 7, 373–379.

Liu, Q.R., Nelson, H., Mandiyan, S., Lopez-Corcuera, B., Nelson, N., 1992. Cloning and expression of a glycine transporter from mouse brain. FEBS Lett. 305, 110–114.

Lopez-Corcuera, B., Vazquez, J., Aragon, C., 1991. Purification of the sodium- and chloride-coupled glycine transporter from central nervous system. J. Biol. Chem. 266, 24809–24814.

Lopez-Corcuera, B., Geerlings, A., Aragon, C., 2001. Glycine neurotransmitter transporters: an update. Mol. Membr. Biol. 18, 13–20.

Lynch, J.W., 2004. Molecular structure and function of the glycine receptor chloride channel. Physiol. Rev. 84, 1051–1095.

Mahendrasingam, S., Wallam, C.A., Hackney, C.M., 2003. Two approaches to double post-embedding immunogold labeling of freeze-substituted tissue embedded in low temperature Lowicryl HM20 resin. Brain Res. Brain Res. Protoc. 11, 134–141.

Martinez-Maza, R., Poyatos, I., Lopez-Corcuera, B., Nunez, E., Gimenez, C., Zafra, F., Aragon, C., 2001. The role of N-glycosylation in transport to the plasma membrane and sorting of the neuronal glycine transporter GLYT2. J. Biol. Chem. 276, 2168–2173.

Muth, T.R., Ahn, J., Caplan, M.J., 1998. Identification of sorting determinants in the C-terminal cytoplasmic tails of the gamma-aminobutyric acid transporters GAT-2 and GAT-3. J. Biol. Chem. 273, 25616–25627.

Ohno, K., Koroll, M., El Far, O., Scholze, P., Gomeza, J., Betz, H., 2004. The neuronal glycine transporter 2 interacts with the PDZ domain protein syntenin-1. Mol. Cell. Neurosci. 26, 518–529.

Pfeiffer, F., Simler, R., Grenningloh, G., Betz, H., 1984. Monoclonal antibodies and peptide mapping reveal structural similarities between the subunits of the glycine receptor of rat spinal cord. Proc. Natl. Acad. Sci. U. S. A. 81 (22), 7224–7227.

Pow, D.V., Hendrickson, A.E., 1999. Distribution of the glycine transporter glyt-1 in mammalian and nonmammalian retinae. Vis. Neurosci. 16, 231–239.

Poyatos, I., Ponce, J., Aragon, C., Gimenez, C., Zafra, F., 1997. The glycine transporter GLYT2 is a reliable marker for glycine-immunoreactive neurons. Brain Res. Mol. Brain Res. 49, 63–70.

Poyatos, I., Ruberti, F., Martinez-Maza, R., Gimenez, C., Dotti, C.G., Zafra, F., 2000. Polarized distribution of glycine transporter isoforms in epithelial and neuronal cells. Mol. Cell. Neurosci. 15, 99–111.

Schroder, M., Kaufman, R.J., 2005. ER stress and the unfolded protein response. Mutat. Res. 569, 29–63.

Shimkus, M., Levy, J., Herman, T., 1985. A chemically cleavable biotinylated nucleotide: usefulness in the recovery of protein-DNA complexes from avidin affinity columns. Proc. Natl. Acad. Sci. U. S. A. 82, 2593–2597.

Smith, K.E., Borden, L.A., Hartig, P.R., Branchek, T., Weinshank, R.L., 1992. Cloning and expression of a glycine transporter reveal colocalization with NMDA receptors. Neuron 8, 927–935.

Stowell, J.N., Craig, A.M., 1999. Axon/dendrite targeting of metabotropic glutamate receptors by their cytoplasmic carboxy-terminal domains. Neuron 22, 525–536.

Torres, G.E., Yao, W.D., Mohn, A.R., Quan, H., Kim, K.M., Levey, A.I., Staudinger, J., Caron, M.G., 2001. Functional interaction between monoamine plasma membrane transporters and the synaptic PDZ domain-containing protein PICK1. Neuron 30, 121–134.

Tsai, G., Ralph-Williams, R.J., Martina, M., Bergeron, R., Berger-Sweeney, J., Dunham, K.S., Jiang, Z., Caine, S.B., Coyle, J.T., 2004. Gene knockout of glycine transporter 1: characterization of the behavioral phenotype. Proc. Natl. Acad. Sci. U. S. A. 101, 8485–8490.

Yee, B.K., Balic, E., Singer, P., Schwerdel, C., Grampp, T., Gabernet, L., Knuesel, I., Benke, D., Feldon, J., Mohler, H., Boison, D., 2006. Disruption of glycine transporter 1 restricted to forebrain neurons is associated with a procognitive and antipsychotic phenotypic profile. J. Neurosci. 26, 3169–3181.

Zafra, F., Aragon, C., Olivares, L., Danbolt, N.C., Gimenez, C., Storm-Mathisen, J., 1995a. Glycine transporters are differentially expressed among CNS cells. J. Neurosci. 15, 3952–3969.

Zafra, F., Gomeza, J., Olivares, L., Aragon, C., Gimenez, C., 1995b. Regional distribution and developmental variation of the glycine transporters GLYT1 and GLYT2 in the rat CNS. Eur. J. Neurosci. 7, 1342–1352.